

---

# Generative Adversarial Network Architectures For Image Synthesis Using Capsule Networks

---

**Yash Upadhyay**

University of Minnesota, Twin Cities  
 Minneapolis, MN, 55414  
 upadh034@umn.edu

**Paul Schrater**

University of Minnesota, Twin Cities  
 Minneapolis, MN, 55414  
 schrater@umn.edu

## Abstract

In this paper, we propose Generative Adversarial Network (GAN) architectures using Capsule Networks for conditional and random image-synthesis. Capsule Networks encode meta-properties and spatial relationships between the features of the image, which helps it become a more powerful critic in comparison to the Convolutional Neural Networks (CNNs) used in current architectures for image synthesis. Our architectures use losses analogous to Wasserstein loss and Capsule Networks, which prove to be a more effective critic in comparison to CNNs. Thus, our proposed GAN architectures learn the data manifold much faster and therefore, show significant reduction in the number of training samples required to train when compared to the current work horses for image synthesis, DCGANs and its variants which utilize CNNs as discriminators. Also, our architecture generalizes over the datasets' manifold much better because of dynamic routing between capsules which is a more robust algorithm for feature globalization in comparison to max-pooling used by CNNs. This helps synthesize more diverse, yet visually accurate images. We have demonstrated the performance of our architectures over MNIST, Fashion-MNIST and their variants and compared them with the images synthesised using Improved Wasserstein GANs that use CNNs.

## 1 Introduction

Generative Adversarial Networks (Goodfellow et al. [2]) are finding popular applications as generative models in diverse scenarios. One of the biggest advantages of GANs is that they can be trained completely using backpropagation. GANs utilize two adversary multi-perceptron networks (generator and discriminator) that play a minimax game where the generator tries to learn the probability distribution  $p_g$  over a dataset  $x$ . Noise variables  $p_z(z)$  serve as an input to the mapping function, the generator,  $G(z, \theta_g)$  with parameters  $\theta_g$ .  $D(x, \theta_d)$  represents the discriminator with parameters  $\theta_d$  and  $D(x)$  represents the probability that the input  $x$  came from the dataset rather than  $p_g$ . Following equation describes the minimax game being played by the adversaries,

$$\min_G \max_D \mathbb{E}_{x \sim p_{data}(x)} [\log(D(x))] + \mathbb{E}_{z \sim p_z(z)} [\log(1 - D(G(z)))] \quad (1)$$

Salimans et al. [12] discussed the problem of simultaneous gradient-descent based training of the discriminator and generator, as proposed by Goodfellow et al. [2], to find a Nash equilibrium. The adversary models update their costs independently, thus, leading to lack of guarantee for convergence. Owing to such issues, there have been multiple iterative developments in the training methods for GANs. Arjovsky et al. [1] discussed how the GAN loss uses Jensen-Shannon divergence as a metric and can be improved upon by using the Earth-Mover's distance and introduced Wasserstein-GAN (WGAN) to alleviate some of the issues with GAN training. But, WGANs used gradient clipping as

a naive way to hold 1-Lipschitz continuity, which was later on improved by Gulrajani et al. [3] with the use of gradient penalty.

While there are many variants of the basic GAN architecture, the core ideas have crystallized and recent innovations revolve around specializing GANs to aid in very specific applications. For example, Kastaniotis et al. [5] have developed an Attention-Aware GAN that uses attention-transfer in order to put emphasis on regions of interest in the cell images they aim to reproduce. He et al. [4] have developed an architecture that can generate visually realistic images with specified attributes by introducing attribute classification constraints rather than putting attribute based constraints on the latent space representation of an image. However, despite the vast differences in the applications of the diverse variety of GANs, most of them which deal with image synthesis are derivatives of the Deep Convolutional GANs or DCGANs (Radford et al. [10]).

Deep Convolutional Neural Networks (LeCun et al. [8]) have been the work-horses for the task of image synthesis for a while (DCGANs, Radford et al. [10]) which use Convolutional Neural Networks or CNNs (Lecun et al. [7]) as discriminators and Deconvolutional Neural Networks (Zeiler et al. [14]) as generators. CNNs capture localized features through the layers over varying granularity and use max-pooling to incorporate positional invariance of these features captured in an image. Despite providing the required variance in positions of the local features (in a limited manner), max-pooling leads to a form of lossy compression of the image features. CNNs do not learn features of an image in a way which can enable it to understand the latent properties of the features themselves and the inter-relations between the other features present in the image. This issue of a lossy feature learning was discussed by Sabour et al. [11], which led to the introduction of Capsule Networks for image classification.

Capsule Networks develop the idea of Capsules, which are a group of neurons whose activity vector represents the instantiation parameters of a specific type of entity such as an object and the length of this activity vector represents the probability of the existence of the entity the vector represents. Capsule Networks incorporate positional-equivariance as opposed to positional-invariance between the features of an image by developing the concepts of Dynamic Routing between Capsules, replacing max-pooling. The attention-like algorithm of Dynamic Routing allows Capsules from a given layer to learn the relevant Capsules from the previous layer which affect the given Capsule's properties. This leads to Capsule Networks learning a richer representation of the features present in the images along with the relations between them on a more global scale allowing them to learn a better representation of the data manifold in comparison to the lossy compression due to max-pooling used in CNNs. This translates to the network learning the data representation significantly faster in terms of the data required in comparison to DCGAN and its derivatives which are essentially data hungry as CNNs require more data to learn features owing to its lossy feature aggregation. Also, since max-pooling provides feature non-localization to a limited extent (in comparison to the a better feature globalization due to routing mechanism between Capsule layers), it also leads to the model learning a highly restricted representation of the features in the data resulting in a form overfitting, ultimately leading to learning the image features in a very strict manner which cannot handle even small affine-transformations well. Capsule Networks have demonstrated to be able to handle such data, with unseen diverse small transformations effectively as reported in the paper by Sabour et al. [11].

Using Capsule Networks as a discriminator in a GAN would provide the advantages of learning the actual data manifold in a richer representation and faster (lesser number of training data points), becoming a more powerful discriminator in comparison to a CNN which would ultimately lead to GAN coupled with Wasserstein Loss that can produce visually accurate images using lesser number of training samples with greater diversity in comparison to GANs employing CNNs while also avoiding mode collapse.

Therefore, we propose GAN architectures for conditional and non-conditional image-synthesis that incorporate Capsule Networks in place of CNNs as discriminators. Capsule Network's ability to learn the features of an image and their spatial relationships in a richer manner will allow the GAN architecture to generate visually accurate images requiring lesser training samples to synthesize, while simultaneously tackling the lack of diverse images generated by learning a better, loss-less representation of the data manifold and synthesizing images with greater variations.

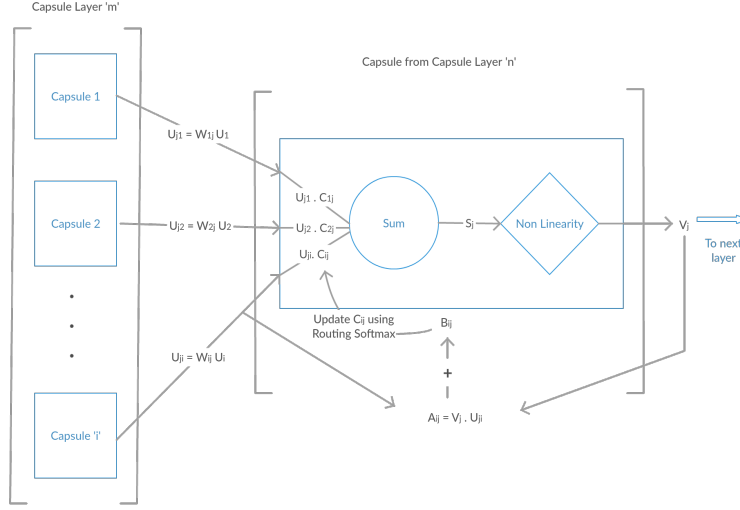


Figure 1: Dynamic Routing between Capsule Network Layers: The figure shows the attention like routing mechanism between capsule layers that allow a capsule to choose its parents via an iterative deterministic process.

## 2 Introduction to Capsule Networks

Sabour et al. [11] developed Capsule Networks as parse trees carved out from a single multi-layer neural network where each layer is divided into many small groups of neurons called as "capsules" corresponding to each node in the parse tree. Each capsule vector represents the meta-properties of the feature/entity the capsule represents and the overall length of the capsule represents the probability of the presence of the entity the capsule represents. Each active capsule chooses its parents from the layer above it using an iterative attention-like routing process. This dynamic routing process replaces the max-pooling step from CNNs allowing for better feature globalization and smarter feature compression.

Since the length of each capsule represents the probability of the presence of the entity it represents, a non-linear "squashing" function is used to shrink the length of this vector between 0 and 1. The output of this non-linearity from capsule  $j$ ,  $v_j$ , is given as follows,

$$v_j = \frac{\|s\|^2}{1 + \|s\|^2} \frac{s_j}{\|s_j\|} \quad (2)$$

where  $s_j$  is the total input.

During the routing process from capsule  $i$  of a given layer to capsule  $j$  of the next layer, the output of capsule  $i$ ,  $u_i$  is first multiplied by the matrix  $W_{ij}$  to give  $u_{ji}$ .  $s_j$  is then calculated as the weighted sum over all  $u_{ji}$  coming from the previous layer to capsule  $j$ , weighted over the coupling coefficient,  $c_{ij}$ .

$$u_{ji} = W_{ij} u_i \quad (3)$$

$$s_j = \sum_i c_{ij} u_{ji} \quad (4)$$

The coupling coefficient  $c_{ij}$  is calculated as the softmax over all  $b_{ij}$ , which is the summation of the agreements,  $a_{ij}$  between the individual input capsules and output of capsule  $j$  over all the iterations.

$$b_{ij} = \sum_t a_{ij_t} \quad (5)$$

$$c_{ij} = \frac{\exp(b_{ij})}{\sum_k \exp(b_{ik})} \quad (6)$$

The Capsule Network introduced by Sabour et al. [11] used a marginal loss over the capsules in the final layer for optimization along with a reconstruction loss which helps in regularization. However, the architectures proposed in this paper do not incorporate the reconstruction loss. The marginal loss,  $L_k$  is defined as following,

$$L_k = T_k(\max(0, m^+ - \|v_k\|^2))^2 + \lambda(1 - T_k)(\max(0, \|v\|^2 - m^-))^2 \quad (7)$$

where  $m^+ = 0.9$ ,  $m^- = 0.1$ ,  $T_k = 1$  iff the entity of class  $k$  is present else,  $T_k = 0$ .  $\lambda = 0.5$  is used as a down-weighting factor to prevent shrinking of activity vectors in the early stages of training.

### 3 Key ideas

Wasserstein Loss maximizes the following objective function as given by Arjovsky et al. [1],

$$\max_{w \in W} \mathbb{E}_{x \sim P_{data}(r)}[f_w(x)] - \mathbb{E}_{z \sim P(z)}[f_w(G_\theta(z))] \quad (8)$$

Here,  $P_{data}$  represents the probability distribution of the dataset and  $P_z$  is the distribution of noise that serves as the input to the mapping function  $G_\theta$ , the generator.  $f_w$  represents the critic that discriminates between real and fake images and gives the probability of the image being real. As explained by Arjovsky et al. [1], the capacity of the critic determines the quality of the gradients provided to the generator and therefore, the faster the critic reaches optimality, the better the generator can be trained. Capsule networks are able to learn the features and the relations between them better than Convolutional Neural Networks because of the attention-like routing mechanism between the capsule layers that allow capsules to deterministically choose the features (or capsules) from the previous layer that affect their values and in turn, the probability of existence of the entity they represent. Convolutional Neural Networks lose the spatial relationships between features through successive layers especially via max-pooling as it brings positional-invariance and proves as a lossy form of feature compression.

The loss we have proposed as a part of the architecture in eqn. 9 and 10, is analogous to Wasserstein Loss and thus, the training is aided by the more powerful critic model. We have experimented and seen that Capsule Networks are indeed faster learners in comparison to Convolutional Neural Networks, as can be seen in Table 1. Thus, coupling these architectural features, it is easy to see why this architecture should perform better and require lesser training epochs.

Also, the fact that each Capsule encodes the properties of the entity/feature it represents allows the architecture to generate more diverse images. This feature of property-encoding makes Capsule Networks robust towards small affine-transformations and thus, accepts synthesized images that resemble the images from the dataset but with small changes. Therefore, it helps the generator learn "healthier" features of the dataset and helps it generate more diverse images in lesser training epochs, something which CNNs cannot do as they do not capture the spatial relationships between the features of the image.

Table 1: Capsule Network v/s Convolutional Neural Network training accuracy comparison(%)

Epochs	MNIST		Fashion-MNIST	
	CNN	CapsNet	CNN	CapsNet
1	91.09	98.51	48.72	84.25
2	93.53	92.22	73.99	86.53
3	95.04	99.41	75.36	87.91
4	95.30	99.58	78.64	88.97
5	95.17	99.63	81.02	90.05

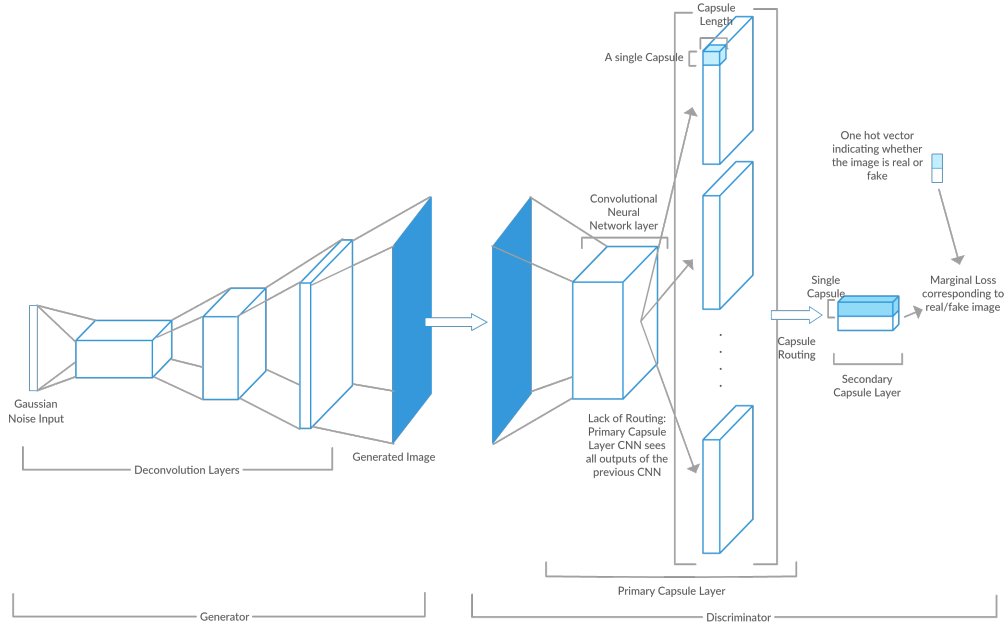


Figure 2: Discriminative Capsule GAN Architecture

## 4 Architectures

In this section, we describe the architectures that this paper proposes for random as well as conditional image synthesis.

### 4.1 Discriminative Capsule GAN architecture for random image synthesis

The generator uses randomly generated latent representation of the image to be synthesized from a Gaussian distribution as the input. The generator consists of a series of deconvolutional neural networks with leaky-relu activations and a tanh activation in the final layer. This is similar to the generator of a DCGAN.

This architecture uses Capsule Networks as a discriminator in place of a Convolutional Neural Network used in DCGANs. It can be seen in Fig. [2], our Capsule Network uses two Capsule layers: Primary and Secondary Capsule layers, in which, there is no routing between the Convolutional layer and the Primary Capsules. Routing exists only between the Primary and Secondary Capsules. The Secondary Capsule layer consists of only two Capsules. The length of the activity vectors of these Capsules represent the probabilities of whether the given image is real or fake.

We combine the marginal losses (eqn. 7) generated by the Capsule Network discriminator from the real and fake images into a loss function which is analogous to the Wasserstein Loss (Arjovsky et al. [1]) as described in eqn. 8. The discriminator loss  $D_l$  and generator loss  $G_l$  are defined as following,

$$D_l = L_{k_{x \sim P(r)}}(x) + L_{k_{x \sim P(z)}}(G_\theta(x)) \quad (9)$$

$$G_l = -L_{k_{x \sim P(z)}}(G_\theta(x)) \quad (10)$$

where  $P(r)$  represents the probability distribution of the real dataset and  $P(z)$  represents the prior distribution serving as the input to the generator  $G_\theta$ .

### 4.2 Split-Auxiliary Conditional Discriminative Capsule GAN

This section describes the architecture developed with Capsule Networks as discriminators to synthesize label specific images.

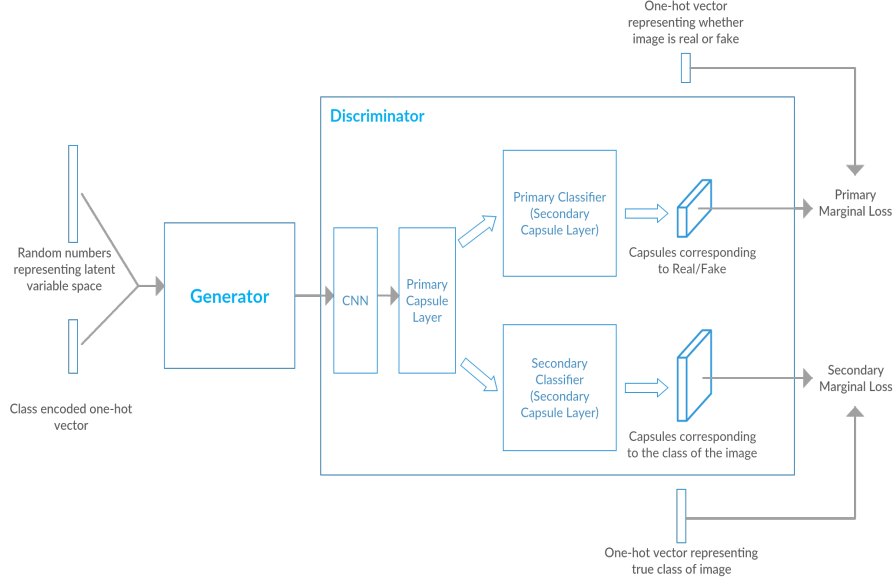


Figure 3: Architecture of Split-Auxiliary Conditional Discriminative Capsule GAN

The generator architecture is similar to the one described in Section 4.1 of this paper. The only difference is in the input to the generator - apart from receiving random variables generated from a Gaussian distribution, the generator also receives the class from which it must synthesize the image. The two vectors are then concatenated and utilized by the generator as a latent space representation of the image to be synthesized.

This discriminator uses a variation of the auxiliary-conditional architecture described by Odena et al. [9]. The discriminator consists of a similar architecture up to the Primary Capsule layer as described in Section 4.1. The Primary Capsules then serve as an input for two different Secondary Capsule layers: Primary Classifier and Secondary Classifier. The Primary Classifier classifies the images into real or fake whereas, the Secondary Classifier classifies the image into the class label it belongs to. The marginal losses (eqn. 7) from the Primary and Secondary Classifiers are used to calculate the Primary Marginal Loss and Secondary Marginal Loss.

Let the Primary Marginal Loss be  $L_{P_k}$  and the Secondary Marginal Loss be  $L_{S_c}$ . The losses for the discriminator ( $D_l$ ) and the generator ( $G_l$ ) is given as follows:

$$D_l = L_{P_k: x \in P(r)}(x) + L_{P_k: x \in P(z)}(G_\theta(x)) + L_{S_c: x \in P(r)|y=c}(x) + L_{S_c: x \in P(z)|y=c}(G_\theta(x)) \quad (11)$$

$$G_l = -L_{P_k: x \in P(z)}(G_\theta(x)) + L_{S_c: x \in P(z)|y=c}(G_\theta(x)) \quad (12)$$

where  $G_\theta$  is the generator with parameters  $\theta$ ,  $P(r)$  corresponds to the probability distribution of the dataset,  $P(z)$  corresponds to the probability distribution of the prior to the generator,  $k \in \{P(r), P(z)\}$ ,  $y$  is the class label of the image, and  $c$  corresponds to the intended class of the image. These are similar to the losses in eqn.(9) and eqn.(10) except for the added Secondary Marginal Loss terms. The Secondary Marginal Losses force the discriminator to learn the representation of an image conditionally over a label. The split architecture allows for the Primary and Secondary Capsule Classifiers to borrow from the same set of extracted features in the Primary Capsules. The Secondary Classifier forces the Primary Capsules to learn what the specific features of the digits and not just the overall features from the dataset, helping the discriminator and generator learn class-specific features faster.

## 5 Experiments

In this section, we evaluate our proposed architectures by comparing them against Improved Wasserstein GAN and Conditional Improved Wasserstein GAN for random and conditional image-synthesis

respectively.<sup>1</sup>The mentioned architectures are being used for comparisons because they architecturally differ only on the discriminator. The generators used by our architectures and the Wasserstein GANs are the same and the loss functions despite being different (incorporating the marginal losses from the Capsule Networks) are analogous to the Wasserstein Loss.

## 5.1 Discriminative Capsule GAN v/s Wasserstein DCGAN

In this section, we have implemented and compared the results between Improved Wasserstein Loss based DCGAN (Gulrajani et al. [3]), that uses gradient penalty instead of gradient clipping to keep the gradients close to a magnitude of 1, and our architecture, Discriminative Capsule GAN. Both the architectures had a learning rate of 0.0002 and mini-batch size of 128. We have trained and compared the performance of the two GANs on MNIST (LeCun [6]) and Fashion-MNIST (Xiao et al. [13]) datasets. To demonstrate the improvement in the overall GAN performance, we have trained a generator with the same parameters in both the architectures. The generator consists of four deconvolutional layers with leaky-relu activation layers having a gradient coefficient of 0.2 and a final deconvolutional layer with tanh activation which results in the image size of  $28 \times 28$ . 100 randomly generated variables from a Gaussian distribution with mean = 0 and standard deviation = 1 serve as input to the generator.

### 5.1.1 Improved Wasserstein DCGAN discriminator implementation details

The discriminator consists of four convolutional layers with leaky-relu activation layers having a gradient coefficient of 0.2 and a final convolutional layer with no non-linear activation applied. Wasserstein Loss (Arjovsky et al. [1]) is used and is coupled with a gradient penalty (Gulrajani et al. [3]) to maintain 1-Lipschitz continuity.

### 5.1.2 Capsule Network discriminator implementation details

The Capsule Network takes images of size  $28 \times 28$  as input and passes them through a convolutional layer having 256 kernels with a stride of 1 and leaky-ReLu activation. The feature maps are then passed on to the Primary capsule layer that forms  $32 \times 6 \times 6$  capsules each having 8 dimensions. These are then routed to the Secondary Capsule layer which consists of 2 capsules of 16 dimensions, one representing the image being real and the other, being fake.

### 5.1.3 Results

In Fig. 4, we can see that within just 5 epochs on both, MNIST and Fashion-MNIST, our architecture has started to give very sharp images in comparison to that of Improved Wasserstein DCGAN. A starker difference is seen on the images generated from Fashion-MNIST dataset. Discriminative Capsule GAN has been able to generate intricate details of over the clothings and handbags whereas, Improved Wasserstein DCGAN is quite far in terms of details from the results that our architecture has produced. In Fig. 5, we can see that despite having visually superior results, our architecture consistently has higher nearest neighbour distances in the Fashion-MNIST dataset in comparison to that of images produced by Improved WGAN. We suggest that this is because our architecture is producing visually superior yet diverse images. As mentioned in Section 3, Capsule Networks are robust to small transformations and thus, classify images synthesized by the generator which have small difference that the original data as real while not classifying images deviating greatly from the dataset as real.

## 5.2 Split-Auxiliary Conditional Discriminative Capsule GAN v/s Conditional Improved Wasserstein DCGAN

In this section, we compare the performance of a Conditional Wasserstein DCGAN with Gradient Penalty (Gulrajani et al. [3]) with that of our architecture. Both the architectures had a learning rate of 0.0002 and a mini-batch size of 128. We tested the architectures on MNIST (LeCun [6]), Fashion-MNIST (Xiao et al. [13]), a dataset of MNIST images rotated with  $0^\circ$ ,  $90^\circ$ ,  $180^\circ$  and  $270^\circ$

---

<sup>1</sup>Implementations can be found at: <https://github.com/yash-1995-2006/Conditional-and-nonConditional-Capsule-GANs/>

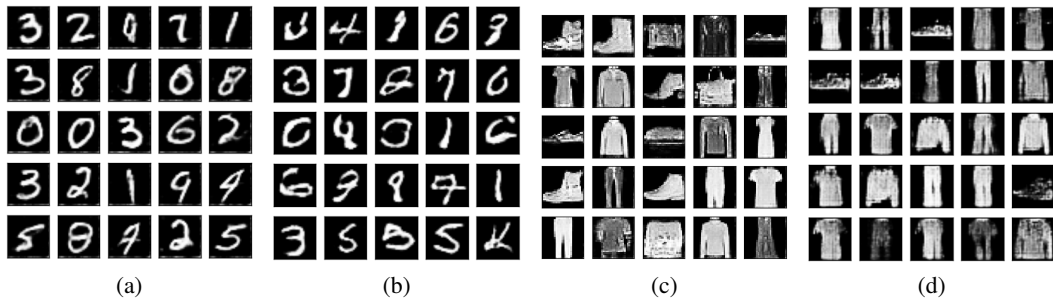


Figure 4: Images generated by the two architectures on 5 epochs (a) Discriminative Capsule GAN trained on MNIST (b) Improved Wasserstein DCGAN trained on MNIST (c) Discriminative Capsule GAN trained on Fashion-MNIST (d) Improved Wasserstein DCGAN trained on Fashion-MNIST. We can see that training Discriminative Capsule GANs for just 5 epochs gives significantly better visual results. It is able to capture the features and details of the dataset in significantly less number of training iterations as opposed to the current architectures.

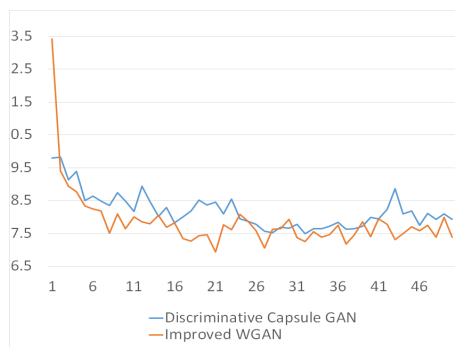


Figure 5: Comparison between Discriminative Capsule GAN and Improved WGAN on basis of mean nearest neighbour distance of images generated every epoch over Fashion-MNIST dataset. The mean distances of images synthesized from our architecture (red) are consistently higher in comparison to the distances of the images synthesized by WGAN (blue) through the epochs despite the fact that they are visually better. Capsule Network is able to capture the features of the images in a much smarter manner in comparison to CNNs, which allows the generator to develop "valid" images with small affine-transformations leading to greater mean nearest-neighbour distances and greater image diversity.

anticlockwise rotations and a dataset of original and horizontally flipped (mirror image) Fashion-MNIST images and compared their results. Both the GAN architectures use generators with the same parameters. The Generator architecture is the same as the one described in Section 5.1. As mentioned in Section 4.2, the only difference is that the input latent variables are conditionally concatenated with the class label representations. 100 random variables coming from a Gaussian distribution having mean=0 and standard deviation = 1 serve and a 10-D one-hot vector representation of the class label serve as the input for the generator.

### 5.2.1 Conditional Improved-Wasserstein DCGAN Discriminator implementation details

The discriminator consist of 4 convolutional layers with leaky-Relu activation layers having a gradient coefficient of 0.2 and a final convolutional layer with no non-linearity applied. This architecture uses a Wasserstein loss Arjovsky et al. [1] with gradient penalty to maintain 1-Lipschitz continuity. The image is conditionally concatenated with the class label to which the image belongs to and the output is a logit which determines whether the image is real or fake.



### 5.2.2 Split-Auxiliary Conditional Discriminative Capsule implementation details

The Capsule Network takes images of size  $28 \times 28$  and passes them through a convolutional layer having 256 kernels with a stride of 1 and leaky-ReLu activation. The feature maps are then passed on to the Primary capsule layer that forms  $32 \times 6 \times 6$  (total 1152) capsules of 8 dimensions. These Capsules are then routed to the Primary Classifier and the Secondary Classifier. Primary Classifier is a secondary Capsule layer that gives 2 16-D capsules, whereas the Secondary Classifier is a secondary Capsule layer that gives 10 16-D Capsules. The capsule values in the Primary Classifier and the Secondary Classifier are determined by dynamic routing from the Primary Capsules. The length of the activity vectors of the Primary Classifier represent the probability of the image being real/fake and the activity vector with the largest length in Secondary Classifier Capsules represents the class of the image with the maximum probability.

### 5.2.3 Results

In Fig. 6, we can see that right from epoch 1, our architecture is able to learn the features of the images and is producing significantly better results than Conditional Wasserstein DCGAN. In Fig. 7, we can see that our architecture despite being trained only over 5 epochs produces images that are visually superior than the images produced by Conditional Wasserstein DCGAN trained over 100 epochs over the rotated MNIST dataset we created. The stark difference in performance can be attributed to the fact that Capsule Networks learn a feature and its spatial arrangement and pose. We can see that our network has learned the difference between a '6' and a '9' despite the rotation by emphasizing upon the curvature of the stem in the '6' and a straight line in case of a '9'. In Fig. 8, we can see that our architecture upon being trained for 10 epochs over flipped Fashion-MNIST produces images of better clarity and detail in comparison to that of images being produced by Conditional Improved Wasserstein DCGAN.

Fig. 9 shows the mean nearest neighbour distance of images of each class and the overall mean nearest neighbour distances over all classes per epoch for images synthesized by Conditional Improved Wasserstein DCGAN and our architecture, Split-Auxiliary Conditional Capsule GAN. In Fig. 9.b, we can see that the nearest neighbour distances come down very fast until epoch 4 and then begin to rise. Despite the increase in the nearest neighbour distance, we can see that the images synthesized are visually clear, pointing to the fact that they are indeed different from the images in the data set that the model has been trained on. The critic has learned the spatial relationships between the features of the data set along the features themselves, giving the generator possibilities to synthesize novel yet not highly deviated images and not be penalized. Whereas on the other hand, Fig. 9.a shows that the nearest neighbour distances of the images synthesized by Conditional Wasserstein DCGAN decrease slowly till epoch 100, becoming smaller than the mean nearest neighbour distances achieved by our model. Paired with the fact that the images generated are visually poorer, we can infer that the model has not been able to completely capture the features and their relationships and is trying to fit the data without providing significant diversity.

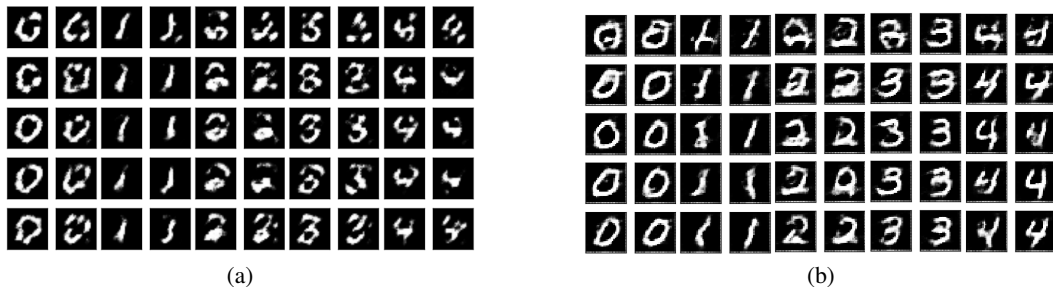


Figure 6: Images generated by (a) Conditional Improved Wasserstein DCGAN and (b) Split-auxiliary Conditional Capsule GAN, trained over MNIST for 1 epoch. Images generated by our architecture show significantly better structure in comparison to the images generated by WGAN after just 1 epoch of training, demonstrating that our model benefited from the faster learning capabilities of the Capsule Networks as the discriminator, owing to its ability to learn the features in the image in a much better manner.

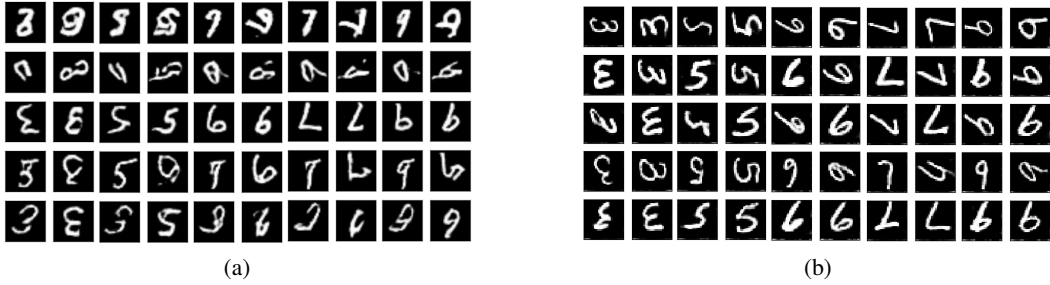


Figure 7: Images generated by (a) Conditional Improved Wasserstein DCGAN trained over MNIST for 100 epochs (b) Split-auxiliary Conditional Capsule GAN trained over MNIST for 5 epochs. The digits being compared are - 3, 5, 6, 7, 9. We can observe that the images generated by our model are visually much better than the images generated by DCGAN despite being trained over significantly lesser number of samples.



Figure 8: Images generated by (a) Conditional Improved Wasserstein DCGAN trained over flipped Fashion-MNIST for 50 epochs (b) Split-auxiliary Conditional Capsule GAN trained over MNIST for 10 epochs. We can observe that despite being trained only over a fraction of training epochs undergone by WGAN, our model was still able to produce better looking results.

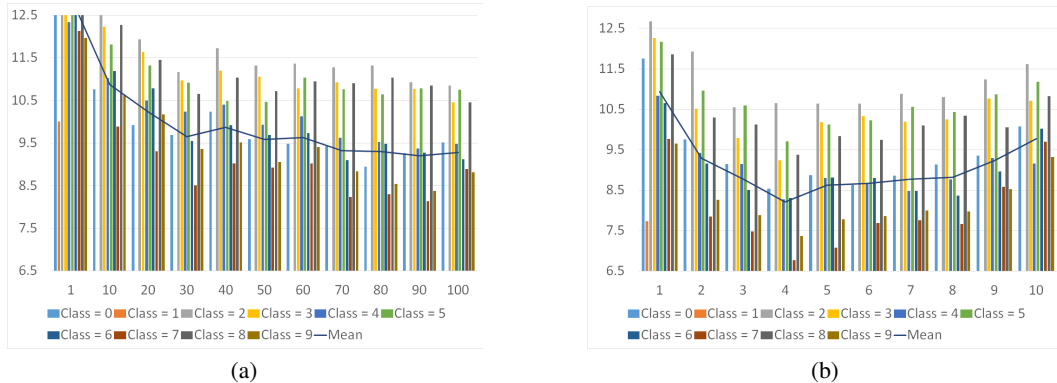


Figure 9: Mean nearest neighbour distances of images generated by (a) Conditional Improved Wasserstein DCGAN trained on rotated MNIST dataset for 100 epochs and (b) Split-Auxiliary Conditional Capsule GAN trained on rotated MNIST dataset for 10 epochs. The nearest neighbour distances in (b) initially go down but end up increasing through the epochs as the model learns the features and leads to better looking images with increased diversity leading to increasing nearest neighbour distances. Whereas, in (a), we can see that despite being trained for 100 epochs, WGAN could not achieve the same visual accuracy as achieved by our architecture, but ends up with lower nearest neighbour distances. This shows that CNNs are relatively slower learners and learn features more superficially, in turn, confining the features that the generator learns.

## 6 Conclusion and Future Work

Capsule Networks have proven to be a great alternative to CNNs as discriminators for GANs as they overcome the problem of lossy feature aggregation for feature non-localization via max-pooling, which leads to CNNs becoming slow learners and completely aloof of meta-features and feature inter-relations. The architecture of capsules and the routing mechanism between them helps Capsule Networks overcome these issues, leading them to learn the transformation manifold of the data in a much better way, further leading it to generalize across the manifold in a much faster.

Our proposed GAN architectures for random and conditional image synthesis, that utilize Capsule Networks as discriminators, outperform the current Generative Adversarial Networks in many ways. Our architectures use losses analogous to the Wasserstein Loss that benefits from the Capsule Network, a more powerful critic in comparison to the conventionally used CNNs for image synthesis, providing healthier gradients to the generator to learn with lesser training data. Meta-features and feature inter-relationships learned by Capsule Networks make them robust to small affine-transformations, leading the generator to synthesize more diverse images in comparison to GANs using CNN discriminators.

The fact that replacing Convolutional Neural Networks with Capsule Networks could bring huge improvements to the overall performance of GANs, points us in a direction which encourages exploration in the application of the concept of capsules to the generator. This would require inverting the Capsule Network tree in such a way that one can derive the instantiation parameters of the features of an image from a smaller number of capsules. Since, the GAN's capability to generate diverse images is limited by the generator's potential, it would make sense to replace Deconvolutional Neural Networks used in today's GANs for image synthesis, with inverse Capsule Networks that learn meta-features and feature-inter-relations which helps the generator to learn features that generalize across the data's manifold, giving it the potential to generate highly diverse images.

## References

- [1] M. Arjovsky, S. Chintala, and L. Bottou. Wasserstein gan. *arXiv preprint arXiv:1701.07875*, 2017.
- [2] I. Goodfellow, J. Pouget-Abadie, M. Mirza, B. Xu, D. Warde-Farley, S. Ozair, A. Courville, and Y. Bengio. Generative adversarial nets. In *Advances in neural information processing systems*, pages 2672–2680, 2014.
- [3] I. Gulrajani, F. Ahmed, M. Arjovsky, V. Dumoulin, and A. C. Courville. Improved training of wasserstein gans. In *Advances in Neural Information Processing Systems*, pages 5769–5779, 2017.
- [4] Z. He, W. Zuo, M. Kan, S. Shan, and X. Chen. Arbitrary facial attribute editing: Only change what you want. *arXiv preprint arXiv:1711.10678*, 2017.
- [5] D. Kastaniotis, I. Ntinou, D. Tsourounis, G. Economou, and S. Fotopoulos. Attention-aware generative adversarial networks (ata-gans). *arXiv preprint arXiv:1802.09070*, 2018.
- [6] Y. LeCun. The mnist database of handwritten digits. <http://yann.lecun.com/exdb/mnist/>, 1998.
- [7] Y. Lecun, L. Bottou, Y. Bengio, and P. Haffner. Gradient-based learning applied to document recognition. *Proceedings of the IEEE*, 86(11):2278–2324, Nov 1998. ISSN 0018-9219. doi: 10.1109/5.726791.
- [8] Y. LeCun, L. Bottou, Y. Bengio, and P. Haffner. Gradient-based learning applied to document recognition. *Proceedings of the IEEE*, 86(11):2278–2324, 1998.
- [9] A. Odena, C. Olah, and J. Shlens. Conditional image synthesis with auxiliary classifier gans. *arXiv preprint arXiv:1610.09585*, 2016.
- [10] A. Radford, L. Metz, and S. Chintala. Unsupervised representation learning with deep convolutional generative adversarial networks. *arXiv preprint arXiv:1511.06434*, 2015.

- [11] S. Sabour, N. Frosst, and G. E. Hinton. Dynamic routing between capsules. In *Advances in Neural Information Processing Systems*, pages 3859–3869, 2017.
- [12] T. Salimans, I. Goodfellow, W. Zaremba, V. Cheung, A. Radford, and X. Chen. Improved techniques for training gans. In *Advances in Neural Information Processing Systems*, pages 2234–2242, 2016.
- [13] H. Xiao, K. Rasul, and R. Vollgraf. Fashion-mnist: a novel image dataset for benchmarking machine learning algorithms. *arXiv preprint arXiv:1708.07747*, 2017.
- [14] M. D. Zeiler, D. Krishnan, G. W. Taylor, and R. Fergus. Deconvolutional networks. In *Computer Vision and Pattern Recognition (CVPR), 2010 IEEE Conference on*, pages 2528–2535. IEEE, 2010.